ELSEVIER

International Journal of Mass Spectrometry 188 (1999) 213–224

International Journal of Mass Spectrometry

Chemical kinetics of lanthanum ionization in H_2–O_2–N_2 flames

QingFeng Chen, John M. Goodings*

Department of Chemistry, York University, 4700 Keele Street, Toronto, Ontario M3J 1P3, Canada

Received 6 October 1998; accepted 18 February 1999

Abstract

Trace amounts ($\leq 10^{-6}$ mol fraction) of lanthanum were introduced into five, premixed, fuel-rich, H_2–O_2–N_2 flames at atmospheric pressure in the temperature range 1820–2400 K. Aqueous salt solutions of the metal were sprayed into the premixed flame gas as an aerosol using an atomizer technique. The concentrations of the major neutral species present in flames, believed to be LaO and OLaOH, are linked by the balanced reaction $LaO + H_2O = OLaOH + H$ having an equilibrium constant $K = 0.1859 \exp(-11\,464/T)$, based on a crude estimate of the bond dissociation energy for lanthanum oxide-hydroxide D_0^0(OLa–OH) = 408 ± 40 kJ mol^{-1}. Metallic ions were observed by sampling the flames through a nozzle into a mass spectrometer and, for kinetics purposes, were measured as profiles of ion concentration versus distance (i.e. time) along the flame axis. The ions detected can be represented by an oxide ion series $LaO^+.nH_2O$ ($n = 0-3$ or more); the genuine flame ions are thought to be LaO^+ ($n = 0$) and $La(OH)_2^+$ ($n = 1$), equivalent to protonated OLaOH. The two ions are linked by the fast balanced reaction $LaO^+ + H_2O + M = La(OH)_2^+ + M$, where M is a third body. The major ion production processes appear to be the chem-ionization reaction $OLaOH + H \rightleftarrows La(OH)_2^+ + e^-$, and thermal (collisional) ionization $LaO + M \rightleftarrows LaO^+ + e^- + M$ because the ionization energy $IE_0^0(LaO) = 4.90$ eV is low. Ion loss processes involve dissociative electron–ion recombination. When electron-ion recombination of $LaO^+.nH_2O$ was made dominant by the trace addition of potassium, values of the global recombination coefficient are given by $(1718 \pm 515)T^{-3.0\pm0.2}$ cm^3 molecule^{-1} s^{-1}. The rate constant for thermal (collisional) ionization of LaO was found to be $8.0 \times 10^{-10}\ T^{1/2} \exp(-IE_0^0/RT)$ cm^3 molecule^{-1} s^{-1}. The pre-exponential factor or cross section is only 8% of that determined for the alkali metals. The rate constant for the chemi-ionization of OLaOH is given by $(5.6 \pm 1.7) \times 10^{-12} \exp(-17\,350/T)$ cm^3 molecule^{-1} s^{-1}. Although no direct evidence was found for particle formation in these flames, both rate constants for ion production would be lower limits if appreciable lanthanum were present as solid particles. (Int J Mass Spectrom 188 (1999) 213–224) © 1999 Elsevier Science B.V.

Keywords: Lanthanum; Gas-phase; Flame ionization; Thermal ionization; Mass spectrometry

1. Introduction

Our interest in the flame ionization of lanthanum began in 1994 with its use as a test substance for a new flame-ion mass spectrometer [1]. It was followed by a qualitative study of the ionization of the group 3 (or 3B) metals La, Y, and Sc in H_2–O_2–Ar flames [2], which was extended to include the further lanthanide metals Ce, Pr, and Nd in contrast with La [3]. Very recently, we completed a quantitative study of the chemical kinetics of yttrium ions in well-characterized H_2–O_2–N_2 flames [4]. Lanthanum, like yttrium, is believed to exist in flames not as atomic La but

* Corresponding author. E-mail: goodings@turing.sci.yorku.ca

PII S1387-3806(99)00035-4

Table 1
Properties of the hydrogen–oxygen–nitrogen flames

Property/flame number	2	25	3	4	5
Equivalence ratio ϕ	1.5	1.5	1.5	1.5	1.5
$H_2/O_2/N_2$	2.74/1/2.95	3.0/1/3.5	3.18/1/4.07	3.09/1/4.74	1.5/1/3.55
Total unburnt gas flow ($cm^3\ s^{-1}$)	300	250	250	200	150
Measured flame temperature (K)	2400	2230	2080	1980	1820
Rise velocity in burnt gas ($m\ s^{-1}$)	19.8	18.6	15.6	11.4	8.4
Equilibrium burnt gas composition (mol fractions)					
H_2O	0.346 0	0.306 3	0.275 4	0.255 3	0.224 9
H_2	0.128 6	0.152 7	0.162 2	0.139 0	0.125 9
O_2	0.000 105 7	0.000 007 90	0.000 000 72	0.000 000 18	0.000 000 01
H	0.006 019	0.002 650	0.001 077	0.000 500 8	0.000 141 5
OH	0.003 084	0.000 795 1	0.000 213 0	0.000 088 90	0.000 017 54
O	0.000 094 69	0.000 009 35	0.000 000 99	0.000 000 23	0.000 000 01
N_2	0.515 7	0.537 5	0.561 0	0.605 2	0.649 0
LaO (% of total lanthanum)	92	89	89	87	83
OLaOH (% of total lanthanum	8	11	11	13	17

almost exclusively as metallic compounds, mainly the oxide LaO and the oxide hydroxide OLaOH. The feature of primary interest for lanthanum is the very low ionization energy of LaO with $IE_0^0(LaO) = 4.90 \pm 0.10$ eV [5,6]. The hydrogen flames employed contain very little natural ionization but when they were doped with $\sim 10^{-6}$ mol fraction of lanthanum, strong ion signals were observed compared to those for the same concentration of yttrium. The lanthanum ion signals increased steadily downstream in the flames, especially in those at high temperature; a similar behavior is observed for the alkali metals which have low ionization energies. The inference was that lanthanum ions were produced not only by chemi-ionization, as for yttrium, but also by thermal (collisional) ionization. We are not aware of a previous case in flame ionization where thermal ionization of a molecule is a major process.

Our main objective in the present study was to measure quantitative values of rate constants for production and loss of lanthanum ions. The rate constants for thermal (collisional) ionization of the five alkali metals were found previously to be given by the expression $(9.9 \pm 2.7) \times 10^{-9}\ T^{1/2} \exp(-IE_0^0/RT)$, where IE_0^0 is the ionization energy of the alkali metal atom [7]. The ionization energy of LaO is bracketed by those of sodium and potassium, i.e. $IE_0^0(Na) = 5.139$ and $IE_0^0(K) = 4.34l$ eV [5,6]. It is of considerable interest to see whether the rate constant for thermal ionization of LaO is in line with the expression for the alkali metals because different factors are involved for an atom compared with a molecule. Although $IE_0^0(YO) = 6.0 \pm 0.3$ eV [5,8] (or 5.85 ± 0.15 eV [5,9]) is appreciably higher, the thermal ionization of YO in our previous study of yttrium [4], if present at all, might have accounted for $<1\%$ of the yttrium ionization. Also in that study, the rate constant for the chemi-ionization of yttrium was determined to be $(2.7 \pm 0.8) \times 10^{-12} \exp(-22\ 452/T)\ cm^3\ molecule^{-1}\ s^{-1}$, and it is of interest to compare it with the corresponding value for lanthanum, the next higher metal from the same chemical group. Ion loss processes will involve dissociative electron–ion recombination although the molecular ions can lead to a variety of neutral products.

2. Experimental

Five, premixed, laminar, H_2–O_2–N_2 flames at atmospheric pressure of fuel-rich composition (equivalence ratio $\phi = 1.5$) in the temperature range 1820–2400 K were employed for this work, and their

properties are listed in Table 1. These flames were originally characterised by Kittelson [10] who measured their rise velocities and temperatures in the burnt gas by sodium *D*-line reversal [11] using burner systems essentially identical to ours. Allowing for the slight variation in the measured temperature profiles downstream and the accuracy of the flowmeter settings [10], the temperature in each case is within ± 50 K ($<\pm 3\%$) of the value quoted in Table 1 for the range from 5 to 30 mm downstream of the reaction zone; it is about 65 K lower than the calculated adiabatic flame temperature. The calculated compositions of the equilibrium burnt gas are based on the JANAF Tables [12]. The concentrations of free radicals, primarily H, OH, and O, overshoot their equilibrium values in the reaction zone of each flame and then decay downstream toward equilibrium in the burnt gas; the effect is greater the cooler the flame. The degree of overshoot is specified by Sugden's disequilibrium parameter γ [13] defined as the ratio of the actual concentration of a species at any point in the flame to its equilibrium concentration in the burnt gas given in Table 1. For fuel-rich flames where $[H_2O]$ and $[H_2]$ are constant in the burnt gas, $\gamma_H = \gamma_{OH} \equiv \gamma$ whereas $\gamma_O = \gamma^2$. For the five flames employed here, Butler and Hayhurst [14] have measured γ as a function of distance z along the flame axis, i.e. the radical concentrations are known at all points in the flames. Even at $z = 30$ mm downstream in flames 3, 4, and 5, $\gamma \neq 1$. All five fuel-rich flames are cylindrical in shape with a diameter of about 12 mm. For purposes of chemical kinetics, they are pseudo-one-dimensional (flat) in plug flow with rise velocities in the burnt gas given in Table 1. The flames are stabilized on a water-cooled brass burner previously described [1].

Lanthanum was introduced into the flames by spraying an aqueous solution of a lanthanum salt into the premixed flame gas as an aerosol derived from an atomizer described previously [15], operated by a flow of 16.2 $cm^3\ s^{-1}$ of the diluent nitrogen gas. Spraying a 0.1 M solution introduced 9.5×10^{-7} mol fraction of total metal into a premixed flow of 250 $cm^3\ s^{-1}$. The atomizer calibration departs from linearity when the solution concentration exceeds roughly 0.2 M. The lanthanum-doped flames were pale green in colour with a bluish reaction zone near the burner face. In some cases, it was desirable to introduce potassium along with the lanthanum. A convenient way to change the concentration ratio of the mixed solution was to set up two burettes containing fairly concentrated solutions of the two metallic salts. Aliquots drawn from each, when diluted with distilled water, provided a wide range of concentrations and their ratios. The salts used to make up the solutions were $La(NO_3)_3.6H_2O$ (Aldrich, 99.999%) and KNO_3 (Fisher, >99.9%).

The burner was mounted horizontally on a motorized carriage with calibrated drive coupled to the *X* axis of an *XY* recorder. The flame axis *z* was accurately aligned with the sampling nozzle of the mass spectrometer. Two types of conical sampling nozzles [1] were employed in these studies: one with a tiny electron microscope lens of Pt/Ir alloy swaged into the tip of a stainless steel cone with an orifice diameter of 0.170 mm; and one in the form of a 60°, sharp-edged, electroformed, nickel cone with an orifice diameter of 0.198 mm at the tip. The latter type has a smaller thermal boundary layer such that the formation of ion hydrates is minimized; these hydrates form as a result of the cooling, which occurs during sampling of the flame gas into the mass spectrometer.

The whole apparatus including the mass spectrometer has already been described in detail [1] so that only a brief outline will be given here. Flame gas including ions is sampled into a first vacuum chamber maintained at 0.04 Pa (3×10^{-4} Torr). The ions are formed into a beam by an electrostatic lens, pass through a 3 mm orifice in a nose cone into a second vacuum chamber maintained below 0.003 Pa ($<2 \times 10^{-5}$ Torr), are conditioned by a second ion lens for analysis by a quadrupole mass filter, collected by a parallel-plate Faraday detector, and measured by a sensitive electrometer coupled to the *Y* axis of the *XY* recorder. Ion signal magnitudes measured in the figures given as a voltage (in millivolts) refer to the collected ion current passing through a grid-leak resistor of $10^{10}\ \Omega$. By driving a flame toward the sampling nozzle, the profile of an individual ion signal versus distance along the flame axis *z* can be

obtained. Experimentally, $z = 0$ is defined where the pressure abruptly rises when the sampling nozzle pokes through the flame reaction zone into the cooler unburnt gas upstream. The pressure is obtained from an ionization gauge mounted on the second vacuum chamber. As an alternative to individual ions, total positive ion (TPI) profiles can be measured by switching off the dc voltages to the quadrupole rods. Still with the dc voltages switched off and the spectrometer's mass dial set to a given mass number, all of the ions above that mass are collected; e.g. TPI_{12} designates all of the positive ions (since no measurable flame ion signal exists below 12 u), and TPI_{145} includes all of the lanthanum ions $LaO^+.nH_2O$ (n = 0–3 or more).

3. Results and discussion

3.1. Neutral lanthanum species in flames

The aerosol droplets from the atomizer dry out in the premixed flame gas and enter the burner as crystallites of $La(NO_3)_3.6H_2O$. When the crystallites warm up in the preheat zone and early reaction zone, they dissociate to produce atomic La initially. A subsequent series of fast bimolecular reactions could result in a variety of molecular species including the oxide, hydroxides and oxide-hydroxide; e.g.

$$La + OH \rightarrow LaO + H \quad (1)$$

$$La + H_2O \rightarrow LaO + H_2 \quad (2)$$

$$La + H_2O = LaOH + H \quad (3)$$

$$LaOH + H_2O \rightarrow La(OH)_2 + H \quad (4)$$

$$La(OH)_2 + H_2O \rightarrow La(OH)_3 + H \quad (5)$$

It is assumed that the oxide and oxide-hydroxide are linked by the balanced reaction (denoted by the equals sign)

$$LaO + H_2O = OLaOH + H \quad (6)$$

as was shown to be the case in flames for the group 13 (or 3A) metal aluminum [16], another metal with three valence electrons that has good thermodynamic data available [12]. For aluminum, the monohydroxide AlOH is a fairly major species [16], but not the oxide AlO whose bond strength is much less than that of LaO. Back donation of electron density from the O atom to form the very strong La–O bond argues against the formation of appreciable LaOH. For example, radical attack at the H atom for the production of the oxide is favoured thermodynamically

$$LaOH + H, OH \rightarrow LaO + H_2, H_2O \quad (7)$$

In fact, we have argued previously that none of the neutral lanthanum hydroxides have appreciable concentrations in flames [2]. It is noteworthy that the elimination of water from the higher hydroxides leads back to the oxide and oxide-hydroxide

$$La(OH)_2 \rightarrow LaO + H_2O \quad (8)$$

$$La(OH)_3 \rightarrow OLaOH + H_2O \quad (9)$$

In summary, the available evidence suggests that LaO and OLaOH are the major neutral species in flames, linked by the fast balanced reaction (6); the equilibrium concentrations of atomic La and the hydroxides are assumed to be negligible. A similar conclusion was reached for yttrium [4].

A crude estimate of the relative concentrations of LaO and OLaOH at equilibrium can be made by setting the equilibrium constant $K_6 = \exp(-\Delta G_6^0/RT)$ for reaction (6) with $\Delta G_6^0 = \Delta H_6^0 - T\Delta S_6^0$. For this reaction, $\Delta H_6^0 = D^0(H–OH) - D^0(OLa–OH)$; $D^0(OLa–OH)$ has been previously estimated to be 408 ± 40 kJ mol^{-1} (4.23 ± 0.41 eV) [2] and $D^0(H–OH)$ = 498 ± 4 kJ mol^{-1} [17] (5.16 ± 0.04 eV), giving $\Delta H_6^0 \approx 90$ kJ mol^{-1}. A rough value of $T\Delta S_6^0$ has been estimated from other species in the +3 oxidation state for which thermodynamic data are available in the JANAF Tables [12]. In the temperature range 1820–2400 K, $T\Delta S_6^0$ varies from −30.9 to −39.1 kJ mol^{-1} for aluminum and from −39.5 to −46.8 kJ mol^{-1} for boron. Overall, higher mass favours the smaller absolute value although the translational contribution to ΔS_6^0 for lanthanum is larger. As a compromise in formulating ΔG_6^0 for lanthanum, the ΔS_6^0 values for aluminum at each flame temperature have been assumed, together with the con-

stant value of $\Delta H_6^0 = 90$ kJ mol^{-1}; the dependence of ΔG_6^0 on ΔS_6^0 is not very sensitive. Values of $K_6 = \exp(-\Delta G_6^0/RT)$ were calculated at each flame temperature to give $[OLaOH]/[LaO] = K_6[H_2O]/[H]$; in this temperature range, the least-squares fit of a straight line to a plot of ln K_6 versus $1/T$ yields $K_6 = 0.1859 \exp(-11\,464/T)$. Using $[H_2O]$ and [H] from Table 1, the percentages of total lanthanum present in each flame as [OLaOH] and [LaO] were obtained, and are given at the bottom of Table 1; the metallic ions constitute only a negligible fraction of the total metal present. The percentages range from 8% OLaOH, 92% LaO in the hot flame 2 to 17% OLaOH, 83% LaO in the cooler flame 5. Because reaction (6) involves the radical H, the relative concentrations of the two metallic species depend on the disequilibrium parameter γ, and vary in the burnt gas wherever γ varies. Exactly analogous equations for the γ dependence have already been given for yttrium [4].

3.2. Lanthanum ion reactions in flames

The H_2–O_2–N_2 flames contain only a small degree of natural ionization produced by the chemi-ionization reaction [18]

$$H + H + OH \rightleftarrows H_3O^+ + e^- \quad (10)$$

With H_3O^+, OLaOH and LaO can undergo chemical ionization reactions by proton or electron transfer

$$H_3O^+ + OLaOH \rightleftarrows H_2O + La(OH)_2^+ \text{ or}$$

$$HOLaO.H^+ \quad (11)$$

$$H_3O^+ + LaO \rightleftarrows H_2O + H + LaO^+ \quad (12)$$

both of which are exothermic. We have argued previously for the group 3 (or 3B) metals [2] that the ionization receives an initial boost from the chemi-ionization reaction [19,20]

$$La + O \rightleftarrows LaO^+ + e^- \quad (13)$$

because [La] may be appreciably close to the flame reaction zone and $[O] = \gamma^2[O]_{eq}$. Further downstream, a major source reaction is believed to be the chemi-ionization process [2]

$$OLaOH + H \rightleftarrows e^- + La(OH)_2^+ \text{ or } LaO^+.H_2O \quad (14)$$

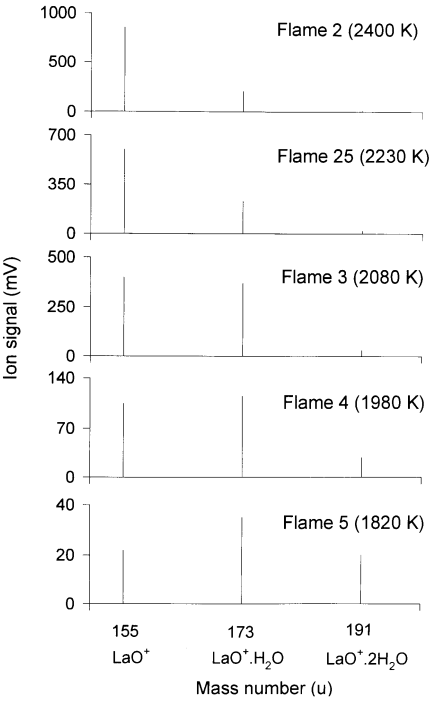

Fig. 1. Mass spectra of the lanthanum ions $LaO^+.nH_2O$ ($n = 0$, 1, and 2) in the five fuel-rich flames measured at $z = 30$ mm downstream for the temperature range 1820–2400 K with the atomizer spraying a 0.05 M solution of $La(NO_3)_3.6H_2O$.

Since the odd electron in LaO is only weakly bound leading to the low value of $IE_0^0(LaO) = 4.90$ eV and since LaO is a major neutral metallic species, thermal (collisional) ionization might be expected to proceed at a high reaction rate

$$LaO + M \rightleftarrows LaO^+ + e^- + M \quad (15)$$

where M is a third body. In general, the two metallic ions can be linked by the fast balanced reaction

$$LaO^+ + H_2O + M = La(OH)_2^+ + M \quad (16)$$

The lanthanum ions observed in each of the five flames are shown in Fig. 1 with the atomizer spraying a 0.05 M solution of $La(NO_3)_3.6H_2O$; the flames were sampled downstream at $z = 30$ mm using a conical nickel nozzle of orifice diameter 0.198 mm. The observed ions can be represented by a hydrate series $LaO^+.nH_2O$ ($n = 0,1,2, \ldots$); the two principal ions are those with $n = 0$ and 1, the latter equivalent to

$La(OH)_2^+$. The total lanthanum positive ion signal TPI_{145} increases with increasing flame temperature as does the ratio $[LaO^+]/[La(OH)_2^+]$. The higher hydrate with $n = 2$ shows a relative increase with decreasing flame temperature but is probably not a genuine flame ion to any extent. Its signal will be enhanced by cooling in the boundary layer at the nozzle during sampling although it could arise by proton transfer to $La(OH)_3$ if the trihydroxide were present. Tiny signals of still higher hydrate ions with $n = 3$ and even 4 have occasionally been observed but they are also ascribed to sampling artefacts. These higher hydrates are produced by fast balanced reactions which should have high rates because H_2O is such a major combustion product

$$LaO^+.(n-1)H_2O + H_2O + M = LaO^+.nH_2O + M \quad (17)$$

where the third body M may, or may not, be required.

Ion loss processes involve dissociative electron–ion recombination. For $La(OH)_2^+$, the back reaction (−14) is appropriate although

$$La(OH)_2^+ + e^- \rightarrow LaO + H_2O \quad (18)$$

might occur in addition. For LaO^+, presumably three-body recombination by reaction (−15) would be slow compared with (−13), the two-body dissociative channel.

3.3. Recombination of lanthanum ions with electrons

In order to measure the rate constant of ion production by both thermal (collisional) and chemi-ionization, it is first necessary to consider their loss by electron–ion recombination. The objectives here were to form a relatively high concentration of lanthanum ions $LaO^+.nH_2O$ rapidly near the flame reaction zone and then to assure that the recombination reaction was dominant downstream in the burnt gas. The global recombination reaction

$$LaO^+.nH_2O + e^- \rightarrow \text{neutral products} \quad (19)$$

is taken to include reaction (−14) and perhaps reaction (18) for $La(OH)_2^+$, as well as reaction (−13) for LaO^+. A small amount of potassium nitrate KNO_3 was added to the atomizer solution to raise the concentration of free electrons in the flames, thereby enhancing the rate of recombination. Potassium atoms are chemically ionized initially by H_3O^+ to some extent [21]

$$H_3O^+ + K \rightarrow K^+ + H_2O + H \quad (20)$$

but progressively ionize further downstream by thermal (collisonal) ionization [7]

$$K + M \rightleftarrows K^+ + e^- + M \quad (21)$$

There is no evidence that potassium interacts with lanthanum by any process other than its effect on recombination through $[e^-]$. It was necessary to adjust the concentrations of both $La(NO_3)_3.6H_2O$ and KNO_3 in the atomizer solution rather carefully so that (i) H_3O^+ disappears quite rapidly downstream to maximize the region in which $LaO^+.nH_2O$ recombination is dominant, and (ii) $LaO^+.nH_2O$ falls to a value near zero at $z = 30$ mm downstream, indicating that lanthanum ion production by both thermal (collisional) and chemi-ionization is negligible.

Figure 2 presents profiles for flame 5 with the atomizer spraying a mixed aqueous solution of 0.0048 M $La(NO_3)_3.6H_2O$ and 0.0015 M KNO_3. At these concentrations, the profiles fulfill the conditions outlined in (i) and (ii). The TPI_{145} signal includes only the lanthanum ions $LaO^+.nH_2O$. Because negative ions are negligible in fuel-rich flames, the TPI_{12} profile that measures the sum of all positive ions gives $[e^-]$ because a flame is a quasi-neutral plasma. From reaction (19), $-d[TPI_{145}]/dt = k_{19}[TPI_{145}][e^-] -$ (ion production term) with $v = dz/dt = 8.4$ m s^{-1} from Table 1. Figure 3 shows a plot of $-vd[TPI_{145}]/dz$ versus $[TPI_{145}][e^-]$ which gives a good straight line in the range $z = 9$–30 mm where k_{19} is the slope; the determination required the measurement of a calibration/conversion factor of 1 mV = 1.142×10^7 ions cm^{-3}. The value of the recombination coefficient $k_{19} = 2.66 \times 10^{-7}$ cm^3 molecule^{-1} s^{-1}. The fact that the straight line passes close to the origin

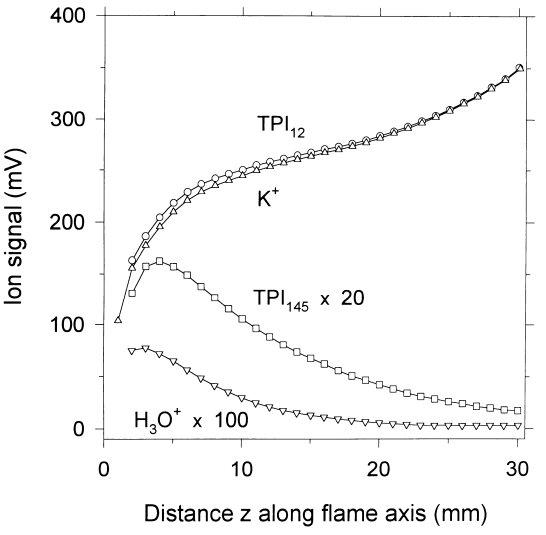

Fig. 2. Ion profiles along the axis of flame 5 with the atomizer spraying a solution of 0.0048 M $La(NO_3)_3.6H_2O$ and 0.0015 M KNO_3 such that electron–ion recombination of the $LaO^+.nH_2O$ ions is the dominant process downstream. The flame reaction zone is located upstream of $z = 0$.

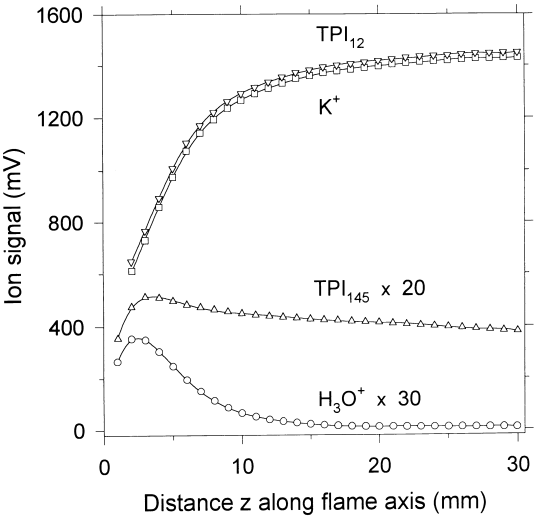

Fig. 4. Ion profiles along the axis of the hot flame 2 with the atomizer spraying a solution of 0.0048 M $La(NO_3)_3.6H_2O$ and 0.0015 M KNO_3 in an unsuccessful attempt to measure electron–ion recombination of the $LaO^+.nH_2O$ ions. The flame reaction zone is located upstream of $z = 0$.

shows that ion production is small under the conditions chosen, in accordance with condition (ii). Experiments were also carried out in which 0.25 mol % of the hydrocarbon CH_4 was added in addition to increase H_3O^+ near the reaction zone in an attempt to raise the TPI_{145} signal by reactions (11) and (12). Although the technique was helpful in our studies of yttrium ion recombination [4], here the lanthanum ion signal was already so large that the CH_4 addition made little difference, and the method was not pursued further.

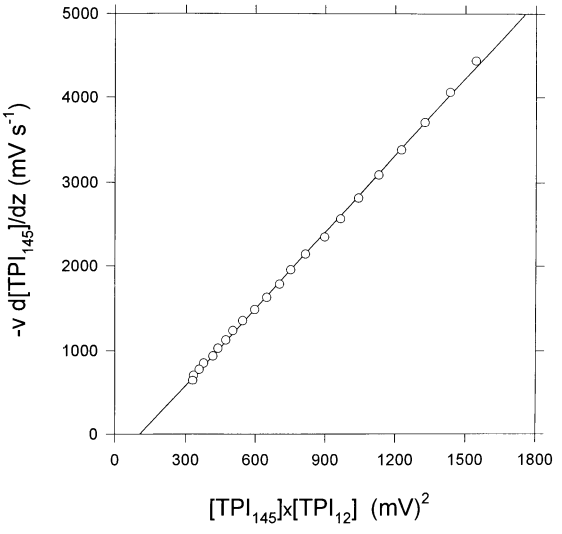

Fig. 3. Recombination plot of $-vd[TPI_{145}]/dz$ vs. $[TPI_{145}] \times [TPI_{12}]$ where $[TPI_{12}] = [e^-]$ in the range $z = 9$–30 mm using the profiles from Fig. 2 for flame 5 with the atomizer spraying a solution of 0.0048 M $La(NO_3)_3.6H_2O$ and 0.0015 M KNO_3.

Values of k_{19} were also measured in flames 4, 3, and 25 but the experiments in flame 2 were not successful, and the ion profiles in Fig. 4 demonstrate this failure. With the atomizer spraying the same mixed solution of 0.0048 M $La(NO_3)_3.6H_2O$ and 0.0015 M KNO_3, the K^+ ion intensity was over 1400 mV but the TPI_{145} signal remained far above zero at $z = 30$ mm downstream, in violation of condition (ii). In Fig. 4, it can be clearly seen that there is still a lot of ion production far downstream. As a consequence, the slope of a recombination plot gave $k_{19} = 3.18 \times 10^{-8}$ cm^3 molecule^{-1} s^{-1}, a value which is too low compared with a typical recombination coefficient of $\sim 1 \times 10^{-7}$ cm^3 molecule^{-1} s^{-1}. When a higher concentration of KNO_3 was used to suppress

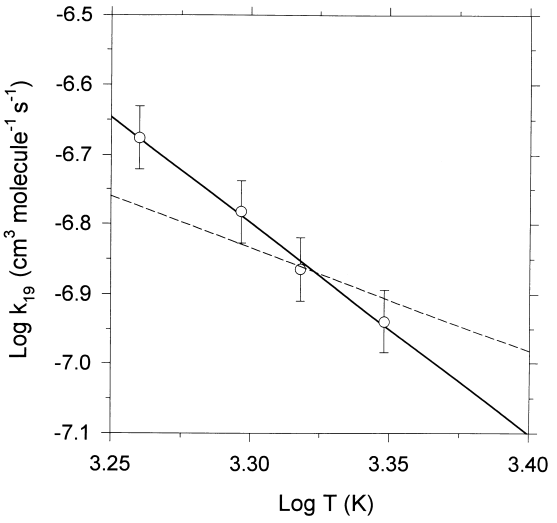

Fig. 5. Logarithmic plot of the global recombination coefficient k_{19} vs. temperature T in the range 1820–2230 K. The solid line fitted by least squares exhibits a $T^{-3.0\pm0.2}$ dependence, for comparison with the dashed line giving the $T^{-1.5}$ dependence expected from simple theory.

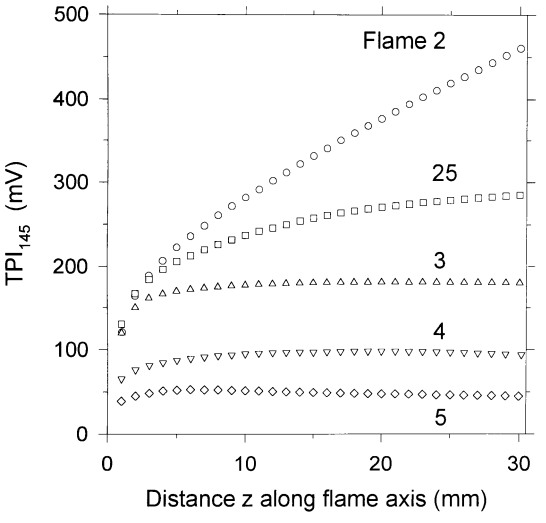

Fig. 6. Total lanthanum ion profiles with the signal measured as TPI_{145} along the axis of the five fuel-rich flames with the atomizer spraying a 0.01 M solution of $La(NO_3)_3.6H_2O$. The flame reaction zone is located upstream of $z = 0$.

the ion production further, "beam spreading" was evident [22,23]. That is, the beam current corresponding to TPI_{12} was so large that it was reduced by the mutual Coulombic repulsion of positive ions in the radial direction causing a low (incorrect) value of TPI_{12}.

The same procedures were carried out for the four fuel-rich flames listed in Table 1 spanning the temperature range from 1820 to 2230 K. The results of many determinations of the recombination coefficient are given in Fig. 5 as a plot of log k_{19} versus log T. The least-squares fit of a straight line through the data points gives $k_{19} = (1718 \pm 515)\ T^{-3.0\pm0.2}$ cm^3 molecule^{-1} s^{-1} with a negative temperature dependence. For flame 2, $k_{19} = 9.10 \times 10^{-8}$ cm^3 molecule^{-1} s^{-1} can be determined from the plot in Fig. 5. Simple theory indicates a $T^{-1.5}$ temperature dependence of the electron–ion recombination coefficient in the context of flames [24]. It is clear that our experimental temperature coefficient for lanthanum ions is higher, although a rather high value of $T^{-2.3\pm0.6}$ was also obtained for the recombination of yttrium ions [4].

3.4. Production of lanthanum ions

Profiles for total lanthanum ionization measured as TPI_{145} are presented in Fig. 6 for the five fuel-rich flames with the atomizer spraying a 0.01 M solution of $La(NO_3)_3.6H_2O$. At this relatively low concentration, each profile rises near the reaction zone but a differing trend in the downstream behaviour is evident. For flames 3, 4, and 5, the ion signal reaches an approximately constant plateau value downstream indicative of equilibrium for ion production and ion loss. This suggests that chemi-ionization is the dominant process in these low-temperature flames in analogy with our previous study of yttrium ionization [4]. For yttrium, it was shown that chemi-ionization was the only reasonable production process to balance the loss of ions by electron–ion recombination. For the hot flames 2 and 25, the lanthanum profile exhibits a steady increase downstream indicative of an additional production process. The obvious production process is thermal (collisional) ionization because the ionization energy of LaO is low, between those of Na and K; a similar profile shape is observed for the alkali metals in these flames [7]. This suggests that

thermal (collisional) ionization plays a major role at high temperature. For the profiles in Fig. 6, $d[TPI_{145}]/dt = k_{14}[OLaOH][H]_{eq}\gamma + k_{15}[LaO][M] - k_{19}[TPI_{145}]^2$ because $[TPI_{145}] \approx [e^-]$; any small contribution from reaction (10), if present, has been ignored. Suppose that the rate constant for thermal ionization of the alkali metals is assumed, i.e., $k_{15} = AT^{1/2}\exp(-IE_0^0/RT)$ cm^3 molecule^{-1} s^{-1} with $A = (9.9 \pm 2.7) \times 10^{-9}$ [7]. As defined, the A factor is a constant, independent of temperature; it departs from the usual definition of the Arrehenius pre-exponential factor where $T^{1/2}$ is included in A. For flames 4 and 5, the left-hand derivative in the kinetic equation was set equal to zero; for flame 3 whose ion profile in Fig. 6 has a very slight upward slope, curve fitting was employed. For all three flames, however, the assumption of the alkali-metal value for k_{15} leads to a value of the chemi-ionization rate constant k_{14} which is negative. This indicates that k_{15} for molecular LaO must be different from that for the atomic alkali metals. If the temperature dependence for thermal ionization is assumed to be the same for the molecule and the atoms, the A factor can be adjusted so that both k_{14} and k_{15} fit the kinetic equation. The fit occurs when A is decreased from 9.9×10^{-9} to 8.0×10^{-10}, i.e., $k_{15} = 8.0 \times 10^{-10}\ T^{1/2}\exp(-IE_0^0/RT)$ cm^3 molecule^{-1} s^{-1} with IE_0^0(LaO) = 4.90 eV. The temperature dependencies of (a) k_{14} for OLaOH, (b) k_{15} for LaO using the original alkali-metal expression, and (c) k_{15} for LaO using the modified expression with reduced A factor are presented in Fig. 7 as plots of ln k versus ln T.

The rate constant k_{14} for chemi-ionization of OLaOH + H was determined in the five fuel-rich flames with the atomizer spraying two different solution concentrations of 0.01 and 0.05 M $La(NO_3)_3.6H_2O$. The results giving the temperature dependence are shown in Fig. 8 as a plot of ln k_{14} versus $1/T$, from which $k_{14} = (5.6 \pm 1.7) \times 10^{-12}\exp(-17\ 350/T)$ cm^3 molecule^{-1}s^{-1}. The expression yields values in the range $(4.1–41) \times 10^{-16}$ cm^3 molecule^{-1} s^{-1} corresponding to 1820–2400 K, respectively, with the expected positive temperature dependence. These values are small compared with those for the chemi-ionization of barium (one atomic number lower than lanthanum) by the reactions Ba + OH and/or BaO + H. The latter has rate constants of $(1.2–16.7) \times 10^{-14}$ cm^3 molecule^{-1} s^{-1} for the same

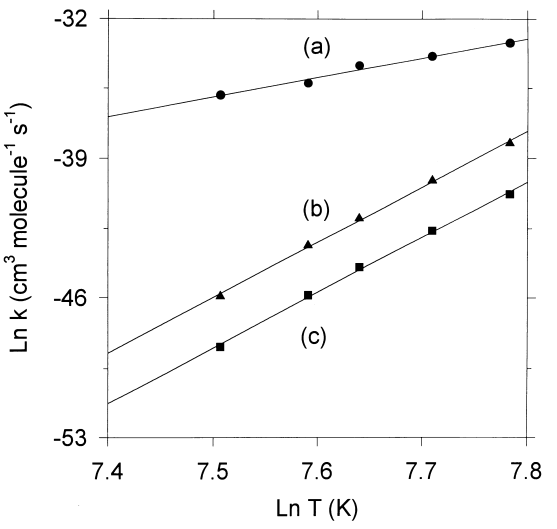

Fig. 7. Logarithmic plots of the rate coefficients k for ion production vs. temperature T: (a) k_{14} for the chemi-ionization of OLaOH + H; (b) k_{15} for the thermal ionization of LaO using the original alkali metal expression; and (c) k_{15} for LaO using the modified expression with reduced pre-exponential factor.

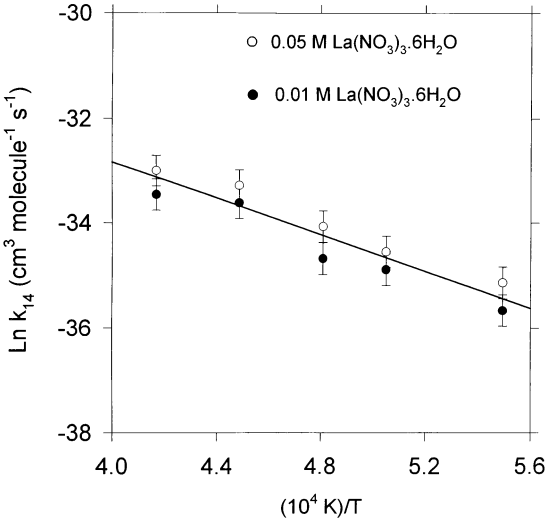

Fig. 8. Semilogarithmic plot of ln k_{14} vs. $1/T$ for the chemi-ionization reaction of OLaOH + H with the atomizer spraying $La(NO_3)_3.6H_2O$ solutions of concentrations 0.01 M (solid circles) and 0.05 M (open circles).

temperature range [23], larger by an approximate factor of 35. However, the values of k_{14} for lanthanum are large compared with those for the similar chemi-ionization reaction of yttrium by OYOH + H, which gives (1.2–23.4) $\times 10^{-17}$ cm^3 molecule^{-1} s^{-1} for the same temperature range [4], smaller by an approximate factor of 25.

3.5. Thermal (collisonal) ionization of LaO

For thermal ionization, the experimental finding that the *A* factor for molecular LaO is only 8% of that for atomic alkali metals warrants further discussion. Hollander et al. [25] proposed and others have discussed [26,27] the flame ionization of the alkalis, as in reaction (21) for potassium, in terms of two elementary steps for a Lindemann process

$$X + M_j \rightleftarrows X^* + M_j \quad (22)$$

$$X^* + M_j \rightarrow X^+ + e^- + M_j \quad (23)$$

where X is ionized by collisions with a partner M_j; in our fuel-rich flames, the dominant collision partners are N_2, H_2O, and H_2. Experimentally for all the alkali metals, the *A* factor in k_{21} is anomalously large, i.e., over a thousand times greater than the gas kinetic value given in braces for $k_{21} = \{(8k/\pi\mu_{X,M})^{1/2}\pi\sigma_{X,M}{}^2\}\ T^{1/2}\exp(-IE^0/RT)$ from simple collision theory; here, *k* is the Boltzmann constant, $\mu_{X,M}$ is the reduced mass, and $\pi\sigma^2_{X,M}$ is the collision cross section for hard spheres. To explain the discrepancy, Hollander et al. [25] proposed a "ladder-climbing" model in which all the electronically excited states of X are thermally populated by reaction (22) in equilibrium with the ground state, and X* is in any one of the very large number of states within $\sim kT$ of the ionization threshold. A final collision of X* produces ionization by reaction (23); experimental evidence suggests that most of these are elastic collisions [26]. Recognize that $kT \sim 0.18$ eV at an average flame temperature of 2100 K. This model appears to provide a satisfactory explanation for the anomalously large *A* factor.

Although the *A* for thermal ionization of LaO is only 8% of that for the alkalis, it is still anomalously large, i.e. approximately a hundred times greater than the gas kinetic value. A mechanism involving reactions (22) and (23) might be applicable with a different "ladder" of energy states that are vibrational rather than electronic. The Morse-type potential energy curves for LaO and LaO^+ are deep; large dissociation energies D^0_0(La–O) = 8.27 eV and D^0_0(O–La^+) = 8.95 eV have been determined for these very strong bonds [28]. Preliminary calculations using the GAUSSIAN 94 programme indicate that the equilibrium internuclear separation of LaO^+ is only slightly smaller than that of LaO, and the vibrational energy spacings are close to 0.1 eV [29,30]. Thus, the LaO^+ curve lies almost directly above that of LaO separated by IE^0_0(LaO) = 4.90 eV; allowing for a slight convergence of the higher vibrational levels, perhaps $v \approx 60$ of LaO might be in approximate coincidence with $v = 0$ of LaO^+. More specifically, two or even three excited vibrational levels of LaO would be within $\sim kT$ of $v = 0$ for LaO^+. The rotational levels of these states would provide a closer energy match. Presumably the conservation of both energy and angular momentum can be satisfied by the separation of the products LaO^+, M_j, and e^-. The cross section or *A* factor for reaction (23) depends on the mutual overlap of the wave functions whose amplitude will be large for $v = 0$ of LaO^+ but very small in the middle Franck–Condon region of $v \approx 60$ for LaO. The actual situation might be helped by the fact that Huber and Herzberg [30] list six electronically excited states of LaO below 4.9 eV, and each may participate in a similar manner. Nevertheless, the very low transition probability for the ionization step when such highly excited vibrational levels are involved does not provide a good basis for an *A* factor about a hundred times greater than the gas kinetic value.

Perhaps a better answer lies in a mechanism very similar to the atomic case involving high-Rydberg states of molecular LaO. The existence of these states is reviewed in a book chapter entitled "High-Rydberg Molecules" by Freund [31]. In the "core ion model" applied to LaO, a highly excited electron in a Rydberg state orbits far away from the LaO^+ ionic core. The

molecular case differs from the atomic one in that the core can have vibrational and rotational excitation, and also can dissociate. In the present case for LaO → LaO^+, dissociation requires much higher energy and therefore is not of primary interest. In one possible scenario, the core ion is in its electronic ground state but is vibrationally excited. "The Rydberg electron, on one of its infrequent passes through the core region, collides superelastically with the core and gains sufficient kinetic energy at the expense of vibrational energy to become ionized. This is called vibrational autoionization" [31]. For any series of energy states between the same two energy limits, the population of each decreases as the number of states increases because the population of the ith state $N_i \propto 1/q$ where q is the total partition function. If the various energies are only loosely coupled, $q = q_t\, q_r\, q_v\, q_e$ for the translational, rotational, vibrational, and electronic contributions. If N_i for an ionizing Rydberg state is compared for LaO and an atom of equivalent mass so that q_t is the same, $(N_i)_{LaO}/(N_i)_{atom} = (q_e)_{atom}/(q_r q_v q_e)_{LaO}$. It is the ratio of the electronic partition functions reduced by q_r and q_v in the denominator. Using data for the ground $X\,^2\Sigma^+$ state of LaO [30] at 2100 K, $q_r = 4140$ and $q_v = 2.34$. The reduction of the cross section or A factor of LaO of 8% of that for an alkali metal would require $(q_e)_{atom} = 775\,(q_e)_{Lao}$. There is an implicit assumption here that the A factor is proportional to the occupation numbers N_i of the high-Rydberg states. From the energy level diagram for an alkali metal [32], it is possible that its q_e is greater than the q_e for LaO but the latter is difficult for us to assess when Rydberg states are involved. Clearly a detailed theoretical study of molecular thermal ionization would be very helpful. We are not aware of other examples for the thermal ionization of a stable molecule having a suitably low ionization energy which are experimentally tractable.

4. Summary and conclusions

The ionization of lanthanum was investigated in five fuel-rich H_2–O_2–N_2 flames. The global electron–ion recombination coefficient of the $LaO^+.nH_2O$ ions (primarily LaO^+ and $La(OH)_2^+$) in the temperature range 1820–2400 K was measured to be $k_{19} = (1718 \pm 515)\ T^{-3.0\pm0.2}$ cm^3 molecule^{-1} s^{-1}, corresponding to values of $2.1–0.9 \times 10^{-7}$, respectively, typical of so many simple molecular ions in flames. The relatively strong $T^{-3.0\pm0.2}$ temperature dependence is significantly different from the $T^{-1.5}$ dependence predicted by simple theory.

Lanthanum ion production appears to occur primarily by way of the chemi-ionization of OLaOH + H in low-temperature flames. As the temperature increases, thermal (collisional) ionization of LaO + M gradually takes over and plays a major role. The percentage ratio of chemi-ionization to thermal ionization is estimated to be 96/4 at 1820 K (flame 5) decreasing to 41/59 at 2400 K (flame 2). This behaviour is in contrast to yttrium ionization where the thermal ionization of YO never exceeds 1% in these flames due to its higher ionization energy, i.e. 5.85 eV instead of 4.90 eV for LaO. At a given temperature in this range, the rate coefficient k_{14} for the group 3 lanthanum chemi-ionization reaction is roughly 35 times smaller than that for the counterpart reaction with barium (BaO + H, or Ba + OH), the adjacent group 2 metal. However, k_{14} is about 25 times larger than that for the same reaction with yttrium, the next lower group 3 metal. Also, the pre-exponential factor or cross section of k_{15} for the thermal ionization of LaO appears to be $<10\%$ of that for the alkali metals. A tentative explanation is discussed involving the high-Rydberg electronic states, but also the rotational and vibrational states, of LaO. Finally, it should be noted that the measured values for both k_{14} and k_{15} would amount to lower limits if any appreciable fraction of the lanthanum metal was present in these flames as solid particles. However, no direct evidence for solid particle formation was found in these studies.

Acknowledgements

The authors would like to thank Professor E.A. Hessels of the Department of Physics, Professors A.C. Hopkinson and H.O. Pritchard of the Department of

Chemistry, York University for helpful discussions concerning the thermal ionization of lanthanum monoxide. Support of this work by the Natural Sciences and Engineering Research Council (NSERC) of Canada is gratefully acknowledged.

References

[1] J.M. Goodings, C.S. Hassanali, P.M. Patterson, C. Chow, Int. J. Mass Spectrom. Ion Processes 132 (1994) 83.
[2] P.M. Patterson, J.M. Goodings, Int. J. Mass Spectrom. Ion Processes 148 (1995) 55.
[3] P.M. Patterson, J.M. Goodings, Int. J. Mass Spectrom. Ion Processes 152 (1996) 43.
[4] Q.F. Chen, J.M. Goodings, Int. J. Mass Spectrom. Ion Processes 176 (1998) 1.
[5] E.P. Hunter, S.G. Lias, NIST Chemistry WebBook, NIST Standard Reference Database Number 69, March 1998 Release (http://webbook.nist.gov/chemistry/ion-ser.htm).
[6] S.G. Lias, J.E. Bartmess, J.F. Liebman, J.L. Holmes, R.D. Levin, W.G. Mallard, J. Phys. Chem. Ref. Data 17 (1988) (Suppl. 1).
[7] A.F. Ashton, A.N. Hayhurst, Combust. Flame 21 (1973) 69.
[8] E. Murad, D.L. Hildenbrand, J. Chem. Phys. 73 (1980) 4005.
[9] E.G. Rauh, R.J. Ackermann, J. Chem. Phys. 60 (1974) 1396.
[10] D.B. Kittelson, Ph.D. Thesis, Cambridge University, 1971.
[11] A.G. Gaydon, H.G. Wolfhard, Flames, 4th ed., Oxford University Press, New York, 1979.
[12] M.W. Chase Jr., C.A. Davies, J.R. Downey Jr., D.J. Frurip, R.A. McDonald, A.N. Syverud, JANAF Thermochemical Tables, 3rd ed., J. Phys. Chem. Ref. Data 14 (1985) (Suppl. 1).
[13] A.N. Hayhurst, D.B. Kittelson, Proc. R. Soc. London, Ser. A 338 (1974) 155.
[14] C.J. Butler, A.N. Hayhurst, J. Chem. Soc., Faraday Trans. 93 (1997) 1497.
[15] J.M. Goodings, S.M. Graham, W.J. Megaw, J. Aerosol Sci. 14 (1983) 679.
[16] P.N. Crovisier, J.H. Horton, C.S. Hassanali, J.M. Goodings, Can J. Chem. 70 (1992) 839.
[17] D.R. Lide (Ed.), CRC Handbook of Chemistry and Physics, 73rd ed., CRC, Boca Raton, FL, 1992.
[18] S.D.T. Axford, A.N. Hayhurst, J. Chem. Soc., Faraday Trans. 91 (1995) 827.
[19] M.C.R. Cockett, J.M. Dyke, A.M. Ellis, T.G. Wright, J. Chem. Soc., Faraday Trans. 87 (1991) 19.
[20] J.M. Dyke, A.M. Shaw, T.G. Wright, in A. Fontijn (Ed.), Gas-Phase Metal Reactions, North-Holland, Amsterdam, 1992, p. 467.
[21] A.N. Hayhurst, N.R. Telford, Trans. Faraday Soc. 66 (1970) 2784.
[22] A.N. Hayhurst, N.R. Telford, Combust. Flame 28 (1977) 67.
[23] J.M. Goodings, P.M. Patterson, A.N. Hayhurst, J. Chem. Soc., Faraday Trans. 91 (1995) 2257.
[24] C.J. Butler, A.N. Hayhurst, J. Chem. Soc., Faraday Trans. 92 (1996) 707.
[25] T. Hollander, P.J. Kalff, C.T.J. Alkemade, J. Chem. Phys. 39 (1963) 2558.
[26] R. Kelly, P.J. Padley, Proc. R. Soc. London, Ser. A 327 (1972) 345.
[27] A.N. Hayhurst, N.R. Telford, J. Chem. Soc., Faraday Trans. 1, 68 (1972) 237.
[28] D.E. Clemmer, N.F. Dalleska, P.B. Armentrout, Chem. Phys. Lett. 190 (1992) 259.
[29] A.C. Hopkinson, R.K. Milburn, Department of Chemistry, York University, Toronto, Canada, private communication, 1998.
[30] K.P. Huber, G. Herzberg, Molecular Spectra and Molecular Structure. IV. Constants of Diatomic Molecules, Van Nostrand Reinhold, New York, 1979.
[31] B.S. Freund, in R.F. Stebbings, F.B. Dunning (Eds.), Rydberg States of Atoms and Molecules, Cambridge University Press, Cambridge, 1983, p. 355.
[32] G. Herzberg, Atomic Spectra and Atomic Structure, Dover, New York, 1944, p. 57.